

A Technique for the Elimination of Stress Waves Overlapping in the Split Hopkinson Pressure bar

S. Wang¹ · E. A. Flores-Johnson² · L. Shen¹

Received: 8 August 2016 / Accepted: 27 March 2017 / Published online: 3 April 2017
© The Society for Experimental Mechanics, Inc 2017

Abstract For valid results in split Hopkinson pressure bar testing, the strain history in the incident bar must be measured at a location where the incident and reflected waves do not overlap. This may prove problematic if the loading pulse is long relative to the length of the incident bar, e.g. due to pulse shaping or when long pressure bars are not available. In this paper an experimental technique for the elimination of overlapping stress waves is presented. By ensuring that the incident wave traverses the bar without noticeable dispersive oscillatory components, a complete pulse history free from superpositioning stress waves can be rapidly constructed via the collation of data from two sets of strain gauges attached at two locations on the incident bar. Experimentation on a sand specimen subsequently validated via finite element modeling demonstrates the advantage of this wave collation technique as it enables the use of longer loading pulses while still satisfying all necessary requirements pertinent to valid Hopkinson bar investigations.

Keywords Split Hopkinson pressure bar · Wave overlapping · Pulse shaping · Finite element simulation

Introduction

The split Hopkinson pressure bar (SHPB) is among the most common devices used for the high strain rate response characterization of engineering materials [1]. Originally developed for the testing of metallic specimens, the SHPB is now increasingly implemented for soft porous materials such as sand and clays [2, 3]. Conceptualized by Hopkinson B [4] and revolutionized by Kolsky H [5] the device enables a means to indirectly extract the mechanical behavior of a specimen sandwiched between two rods (known as the incident and transmission bars). A third rod (the striker bar) is launched at speed into the incident bar which results in the propagation of a compressive stress wave through the pressure bars and specimen. A portion of this pulse is reflected at the specimen/incident bar interface as a tensile wave back towards the impact end of the input bar, while the remaining pulse is transmitted into the specimen.

The incident and reflected strain histories are typically extracted via a strain gauge attached at the midpoint of the incident bar while the transmitted strain history is collected by a gauge on the transmission bar. This effectively communicates the stress and strain histories of the specimen as per equations (1) and (2) respectively, providing that the bars remain linear elastic throughout the test and the dispersion effect is negligible. For a more detailed explanation of such formulations, the reader is referred to Chen and Song [6].

$$\sigma_s(t) = \frac{A}{A_s} E \varepsilon_t(t) \quad (1)$$

$$\varepsilon(t) = \frac{2C_o}{l_s} \int_0^t \varepsilon_r(t) dt \quad (2)$$

where $\varepsilon_r(t)$ and $\varepsilon_t(t)$ respectively denote the reflected and transmitted strain histories, C_o is the bar wave velocity, l_s is

✉ L. Shen
luming.shen@sydney.edu.au

¹ School of Civil Engineering, The University of Sydney, Sydney, NSW 2006, Australia

² CONACYT – Unidad de Materiales, Centro de Investigación Científica de Yucatán, Calle 43, No. 130 Col. Chuburná de Hidalgo, 97200 Mérida, Yucatán, Mexico

the initial specimen length, E is the modulus of elasticity of the bar material and A/A_s denotes the ratio of the bar area to the specimen area.

The extraction of specimen response at high rates of strain via the SHPB relies on the satisfaction of several inherent assumptions. In addition to the requirements of dynamic stress equilibrium and constant rate deformation of the sample, the incident and reflected waves must propagate along the incident bar without overlap at the gauge location. It has been suggested that the pressure bars should be at least twice as long as the striker for a gauge attached at the midpoint [7]. However, this is often not long enough to prevent overlap if the input pulse is altered via pulse shaping, giving rise to the modified SHPB [8]. For the testing of soft or brittle specimens such as foam and sand, it is often required to adopt pulse shaping techniques in conjunction with long striker bars to significantly increase the rise time and thus duration of the input wave in order to effectively achieve dynamic stress equilibrium in the specimen [9–11]. Additionally, under situations where deformations must occur at a constant rate of strain over a large strain range, as opposed to merely a sharp spike characterizing the peak strain rate, the implementation of a long striker bar is often paramount. By increasing the striker length, the plateau sustaining the maximum strain rate can be maintained for longer durations at a given rate of strain, in addition to enabling the extraction of the specimen response at higher strains unattainable via short strikers.

Consequently, the length of the incident bar is often several times longer than the striker if gauges are specified at only the middle of the bar to eliminate the overlapping of stress waves at the gauge location [12]. If overlapping is present, the most direct and intuitive response is to simply adopt a longer incident bar. However, certain practical considerations need to be taken into consideration as the environment of many laboratories configured to support the SHPB testing apparatus may prove problematic. Due to its sheer size, issues such as lack of space or simply the unavailability of alternative bars may eliminate this as a viable option. Subsequently, if a rapid solution is desired or a longer incident bar will only be used for certain types of materials, the procurement of a longer bar may not be economically prudent or time efficient. Additionally, even if longer bars can be sourced, the setup configuration of some laboratories might not be appropriately designed to receive pressure bars beyond a certain length. It therefore becomes necessary to develop procedures to effectively extract the specimen response beyond that of conventional testing.

Previous attempts at addressing this matter pertains to the observation of multiple wave reflections between two strain gauges on the incident bar such as the two-point wave separation technique proposed by Lundberg and Henchoz [13]. The method illustrates the feasibility of multi-gauge strain

sampling under the assumption of one-dimensional wave propagation for pulse travel durations of less than 20 times the distance between the gauges. However, it was concluded that dispersive effects substantially dampen the accuracy of extracted signals for each subsequent wave reflection, thus demonstrating the limitations of the one-dimensional propagation theory [13, 14]. In response, Zhao H, Gary G [15] implemented an iterative approach to effectively extend the duration of a trapezoidal pulse via the observation of strain histories from multiple reverberations at two distinct cross sections on the pressure bars while accounting for wave dispersion. The Pochhammer L [16] and Chree C [17] equations depicting the propagation of longitudinal waves in a bar of infinite length formed the basis of wave separation and the correction of dispersive effects via Fast Fourier Transforms (FFT) in the time domain. The multi-point technique is further optimized by a mathematical method where wave separation is conducted in the frequency domain for all frequencies simultaneously [18]. Henceforth, the adoption of multi-gauge wave separation methods in the context of SHPB testing has proved invaluable in suppressing wave overlap and extending the maximum observable strain for specimens loaded within the intermediate strain rate range (approximately $1\text{--}200\text{ s}^{-1}$) where high strains are difficult to attain otherwise [15, 19].

This paper introduces a simplified approach called here *wave collation* involving the direct reconstruction of recorded strains from gauges attached at two locations on the incident bar for the elimination of overlapping wave trains. The technique differs from classical *wave separation* methods in that it considers only a single reflection of the propagating stress wave in the incident bar (much akin to traditional SHPB tests). In addition, previous wave separation procedures are generally concerned with the extraction of specimen stress-strain behavior at intermediate strain rates not exceeding several hundred [15, 19]. The proposed collation method, on the other hand, is more appropriate for higher strain rates at around 1000 s^{-1} and beyond, as typically achieved via standard Hopkinson bar testing. Under high strain rate conditions, the maximum level of strain observed for any given specimen is expected to be much greater than that loaded under intermediate rates for a single reflection. However, wave overlapping may still manifest especially if modifications such as pulse shaping are adopted to alter the duration of the loading pulse. Hence, the objective is to provide a rapid and simplified procedure which can be implemented for any arbitrary pulse under the high strain rate regime without necessitating complex signal processing on the acquired data. The theory behind the collation technique is introduced in addition to both experimental and numerical validation on a confined sand specimen tested via the modified SHPB. A graph is also provided to aid the design of a SHPB setup in order to accommodate a loading pulse of a given duration.

Theoretical Overview of the Wave Collation Technique for the Mitigation of Overlapping Stress Waves

As previously discussed, a short incident bar may result in the superpositioning of incident and reflected pressure waves. The concept of wave collation is therefore introduced which involves reconstructing the entire incident and reflected strain history via the direct combination of data extracted from strain gauges attached at two distinct locations on the incident bar (referred as Gauges 1 and 2 in Fig. 1). The propagation of a stress wave generated at the impact end of the incident bar is summarized visually via Fig. 2 with inter-gauge travel times relevant to the derivation of the collation equations explored throughout this section denoted.

Data Extraction from Gauge 1

Gauge 1 is designed to capture the entire incident wave without overlap and the front section of the reflected pulse; hence its position is further away from the specimen. The possible maximum duration of the incident wave $T_{i(max)}$ without overlap with its reflected counterpart can therefore be computed. This duration is defined as the time required for a pulse to travel twice the distance from Gauge 1 to the specimen/incident bar interface

$$T_{i(max)} = \frac{2(L_i - d_1)}{C_0} \geq T_i \tag{3}$$

where L_i is the length of the incident bar and d_1 is the distance between the impact end of the incident bar and Gauge 1 (Fig. 1). T_i denotes the duration of any given incident wave, which cannot exceed $T_{i(max)}$ to be free from superpositioning effects. Consequently, the incident wave strain history, $\varepsilon_i(t_i)$ is simply that measured at Gauge 1 (ε_1) across the time

necessary for the pulse to traverse the gauge (equation 4). Given compliance with equation (3), the absence of wave overlap is guaranteed.

$$\varepsilon_i(t_i) = \varepsilon_1(t_i) = \varepsilon_1(0 \leq t_i \leq T_i) \tag{4}$$

Note that the incident wave propagates as a function of time t_i which is taken relative to the beginning of the incident pulse. Subsequently, the non-overlapped duration of the reflected strain history from this gauge, $\varepsilon_1(t_r)$, is defined as the time required for the reflected wave to travel from Gauge 1 to the impact end and back again (covering a distance $2d_1$). Beyond this time mark, the rear portion of the reflected wave will superimpose with its front portion that has been further reflected at the impact end voiding the acquired signal. Hence, the front portion of the reflected signal with $t_r = 0$ denoting its commencement, which has not overlapped with the rear of the reflected wave, is therefore bounded as follows

$$\varepsilon_1(t_r) = \varepsilon_1 \left(0 \leq t_r \leq \frac{2d_1}{C_0} \right) \tag{5}$$

Data Extraction from Gauge 2

While Gauge 1 is only able to capture the leading portion of the reflected wave without overlap, the remaining pulse duration is acquired by Gauge 2. As this gauge is positioned closer to the specimen, the superpositioning of the rear portion of the incident wave and the front portion of reflected wave may occur. This is on account of the reflected signal reaching Gauge 2 before the entire incident wave has had sufficient time to fully traverse the gauge. Hence, it follows that the reflected pulse will only be free of overlapping effects beyond a time corresponding to the time difference between the total incident wave duration (T_i) and the travel time of the incident pulse from

Fig. 1 SHPB schematic showing strain gauges attached at two locations on the incident bar for wave collation

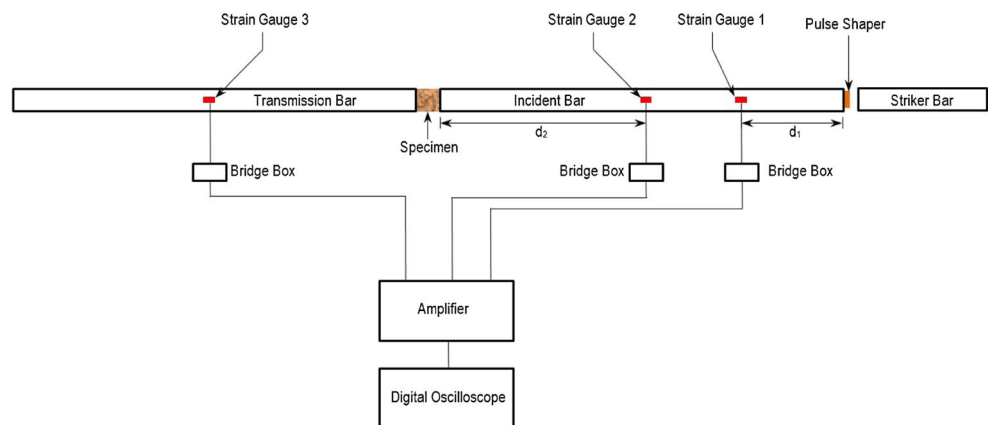
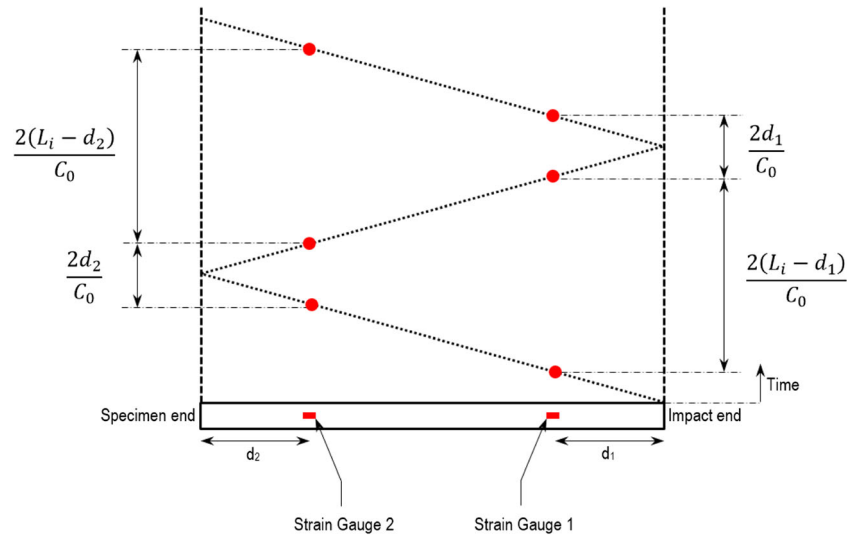


Fig. 2 Stress wave propagation in the incident bar denoting pulse travel times between strain gauges



Gauge 2 to the specimen/incident bar interface and back again (spanning a distance $2d_2$, where d_2 is as per Fig. 1)

$$t_r \geq T_i - \frac{2d_2}{C_0} \tag{6}$$

The maximum valid reflected wave duration without overlapping with itself at Gauge 2 is subsequently governed by the time required for the reflected pulse to travel from the gauge to the impact end of the incident bar and reflected back again, covering a total distance of $2(L_i - d_2)$

$$t_r \leq \frac{2(L_i - d_2)}{C_0} \tag{7}$$

Thus, the valid duration of the reflected strain history as recorded from Gauge 2, $\varepsilon_2(t_r)$ is extracted by combining equations (6) and (7)

$$\varepsilon_2(t_r) = \varepsilon_2 \left(T_i - \frac{2d_2}{C_0} \leq t_r \leq \frac{2(L_i - d_2)}{C_0} \right) \tag{8}$$

Wave Collation Technique

Considering the time boundaries delineated in equations (5) and (6), it is evident that to collate the reflected strain history from both gauges into a single continuous reflected pulse without signal overlap the following condition must hold

$$\frac{2d_1}{C_0} \geq T_i - \frac{2d_2}{C_0} \tag{9}$$

which is rearranged to give

$$\frac{2(d_1 + d_2)}{C_0} \geq T_i \tag{10}$$

Equations (3) and (10) thus present the maximum possible duration for any given loading pulse in order for the wave

collation technique to be successfully implemented. The complete reflected wave strain history without overlapping effects, $\varepsilon_r(t_r)$, can therefore be represented as the combination of strain measurements extracted from Gauges 1 (ε_1) and 2 (ε_2) across their valid time intervals.

$$\varepsilon_r(t_r) = \varepsilon_1(0 \leq t_r \leq \alpha) \cup \varepsilon_2(\alpha < t_r \leq \beta) \text{ for } T_i \leq \left\{ \begin{array}{l} \frac{2(d_1 + d_2)}{C_0} \\ \frac{2(L_i - d_1)}{C_0} \end{array} \right\} \tag{11}$$

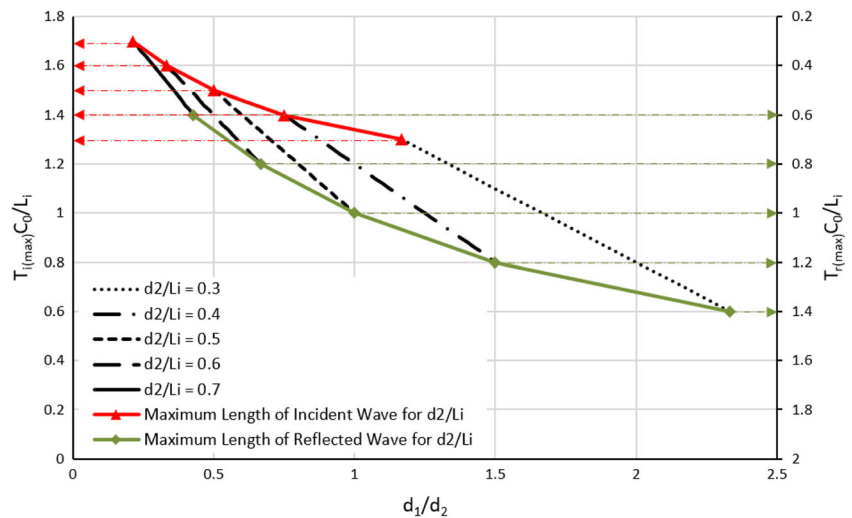
where α is an average between the upper and lower limits of t_r for equations (5) and (8) respectively and β is the upper limit of equation (8)

$$\alpha = \left(\frac{T_i}{2} + \frac{d_1 - d_2}{C_0} \right) \quad \beta = \frac{2(L_i - d_2)}{C_0} \tag{12}$$

Fig. 3 illustrates the relationship between the maximum valid length (pulse duration times wave velocity) of the incident and reflected pulse relative to the incident bar length that can be supported by any given gauge configuration. The procedure for determining such lengths via the graph is summarized as follows:

1. The position of Gauge 2 on the incident bar is selected via its d_2/L_i ratio. This will determine the maximum valid length of the reflected pulse (relative to the length of the incident bar) indicated by the lower curve at the point touching each d_2/L_i line which corresponds with the right y-axis (Fig. 3).
2. The location of Gauge 1 can then be chosen via selecting any point on the d_2/L_i line picked in the previous step. The d_1/d_2 ratio on the x-axis (Fig. 3) governs the positioning of Gauge 1 while the left y-axis denotes the maximum valid length of the incident wave (relative to the length of the incident bar). Both correspond to the chosen point on the d_2/L_i line.

Fig. 3 Theoretical maximum length of incident wave (without overlap) for d_1 and d_2 configurations relative to length of incident bar compared with maximum valid length of reflected wave (without overlap) for d_2 relative to length of incident bar



For a single gauge placed at the midpoint ($d_2/L_i = 0.5$ and $d_1/d_2 = 1$), Fig. 3 stipulates that the maximum incident and reflected wave length the incident bar can support without overlapping is equal to the length of the bar as expected

$$T_{i(max)}C_0 = T_{r(max)}C_0 = L_i \quad (13)$$

where $T_{i(max)}$ and $T_{r(max)}$ is the maximum duration of the incident and reflected waves that an incident bar of length L_i can sustain without overlap represented in equation (3) and the upper bound of equation (8) respectively. If the incident pulse exceeds L_i , a second gauge can extend the effective travel time of the pulse, and the maximum possible duration of the incident wave without overlap increases with decreasing ratios of d_1/d_2 for a given Gauge 2 position. The minimum d_1/d_2 ratio permitted for wave collation is governed by equations (3) and (10) and is represented by the upper optimum curve in Fig. 3. If an even longer incident pulse is to be implemented, Gauge 2 must be shifted closer to the impact end (d_2 must increase). This will however reduce the valid length of the reflected wave as demonstrated via the lower curve in Fig. 3.

As an example, consider that Gauge 2 is placed a distance approximately 35% along the incident bar from the specimen end ($d_2 = 0.35L_i$). The ratio of d_1/d_2 need therefore be minimized to coincide with the upper optimum curve in Fig. 3. For a configuration with $d_2 = 0.35L_i$ and $d_1/d_2 \approx 1.0$, the maximum incident and reflected wave length without overlap is approximately $1.35L_i$ and $1.3L_i$ respectively. This effectively increases the valid duration of the incident and reflected signals by 35% and 30% respectively, when compared with a typical single gauge setup.

Experimental Validation

In order to confirm the veracity of the proposed wave collation technique, the method is implemented on the modified SHPB

test of a confined specimen of silica sand 5 mm thick. The Hopkinson bar configuration is as per Fig. 1 with the incident and transmission bars (manufactured from SKH-51 high strength steel) both 1500 mm long with a diameter of 15 mm. Strain gauges are placed at two locations on the incident bar with $d_1 = 385$ mm and $d_2 = 750$ mm. A 500 mm long 15 mm diameter striker of the same material is used. A hard copper disk 1.02 mm thick with a diameter of 5.5 mm is implemented as a pulse shaper, effectively extending the duration of the incident wave and filtering out high frequency dispersive components.

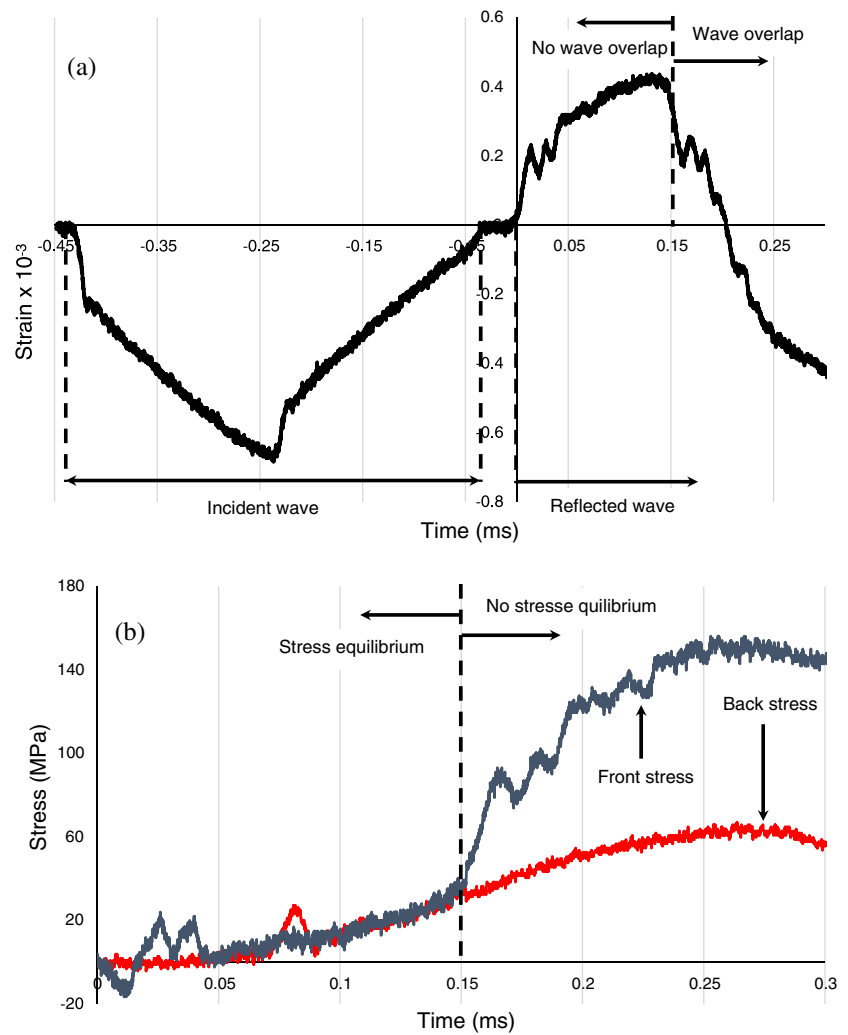
Calibration of Experimental Set-Up

Prior to the implementation of the collation technique, the SHPB configuration must first be calibrated to ensure the valid extraction of experimental data. Evidently, the wave propagation velocity through the bar medium must first be accurately determined for valid SHPB results. This was accomplished by impacting the incident bar with the striker in isolation, without the presence of a specimen or transmitted rod. A series of compressive and tensile stress waves was subsequently extracted from the gauge located at the midpoint of the incident bar. The time interval (Δt) between the start of the compressive pulse and the next reflected compressive pulse was thus used to calculate the wave velocity via the following equation:

$$C_0 = \frac{2L_i}{\Delta t} \quad (14)$$

The wave velocity was consequently determined to be 5195 m/s which closely resembles the theoretical wave propagation velocity derived via $C_0 = \sqrt{E/\rho}$. This subsequently enables the determination of the wave propagation velocity through a specimen (C_s) of a given length

Fig. 4 (a) Incident and reflected wave history, and (b) comparison between specimen front and rear stresses for strains extracted from Gauge 1



(l_s) by observing the time interval (Δt) between the start of the compressive pulse at the midpoint of the incident and transmitted bars:

$$C_s = \frac{l_s}{\Delta t - \frac{L_i + L_t}{2C_0}} \quad (15)$$

Where L_t denotes the length of the transmitted bar. The estimated wave speed of the confined sand specimen was 300 m/s.

Next, the gauges attached at both locations on the incident bar were examined to ensure strain synchronicity. This involved confirming that the gauge factors of the strain gauges were constant such that the corresponding strains converted from their respective voltage measurements were identical for any given amplifier gain. If this condition was violated, the strain histories extracted from the two gauge locations would be desynchronized and the collation procedure could not commence. Equation (16)

denotes the conversion from voltage to strain via two gauges connected to a Wheatstone bridge in the half bridge configuration.

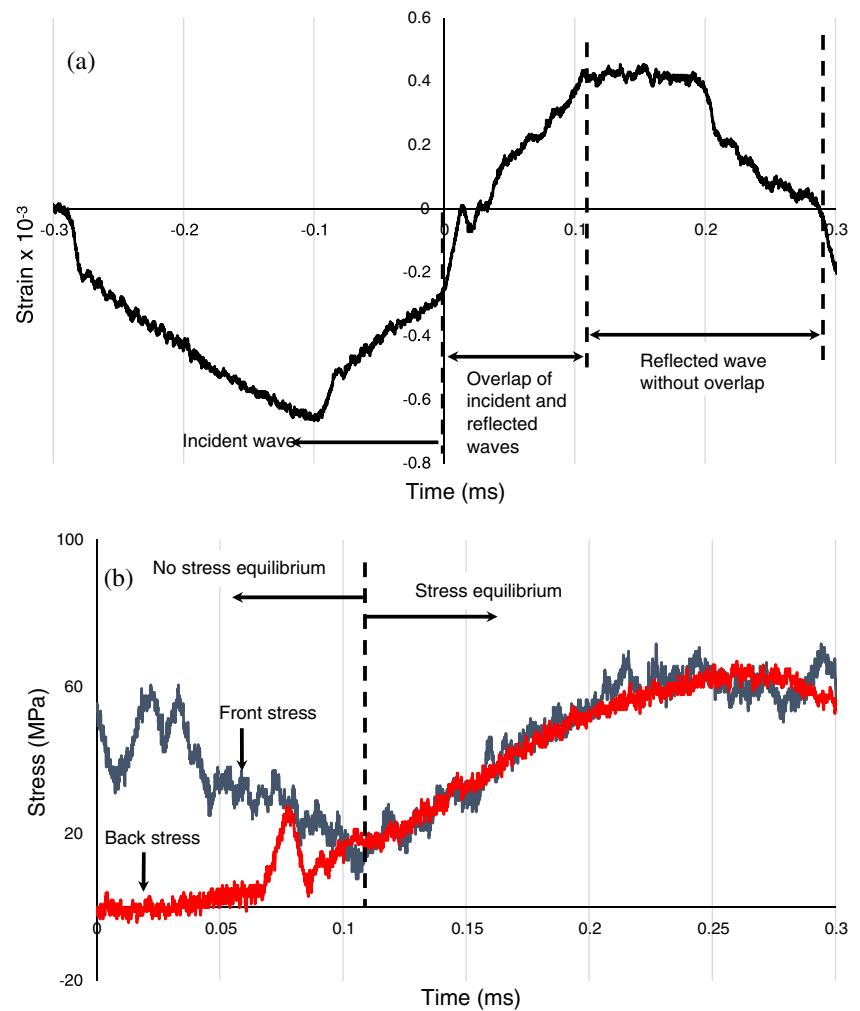
$$\varepsilon = \frac{2V_0}{kV_i} \quad (16)$$

where V_i and V_0 depict the input and output voltages, respectively, and the gauge factor k was stated to be $2.14 \pm 2\%$ by the manufacturer. The strain history derived using equation (16) at both locations on the incident bar was compared and shown to be virtually identical. This confirmed that the gauge factor for both gauges were uniform, enabling the collation of strain data from both gauges to commence.

Data Processing from Gauge 1

Fig. 4(a) displays the strain history collected by Gauge 1 which observes the duration of the incident pulse to be $T_i = 0.4$ ms. Note that due to the application of pulse

Fig. 5 (a) Incident and reflected wave history and (b) comparison between specimen front and rear stresses for strains extracted from Gauge 2



shaping, this duration is significantly longer than the approximate 0.2 ms duration typical for a 500 mm steel striker. Given the bar wave velocity $C_0 = 5195$ m/s, this travel time is far greater than that allowed by a standard mid-bar single gauge setup of 0.29 ms. Compliance for using wave collation is subsequently checked against equations (3) and (10)

$$T_{i(max)} = \frac{2(1.5 - 0.385)}{5195} = 0.43 \times 10^{-3} s \geq T_i \quad (17)$$

$$\frac{2(0.385 + 0.75)}{5195} = 0.44 \times 10^{-3} s \geq T_i \quad (18)$$

The wave collation technique can therefore be implemented. Equation (5) also demarcates the upper time boundary as 0.15 ms until which the reflected wave collected at Gauge 1 is valid. This can be visualized both in the reflected wave time history (Fig. 4(a)) and the stress comparison between both ends of the specimen (Fig. 4(b)). It is evident that the front and back stresses begin to significantly deviate beyond the 0.15 ms time mark as predicted.

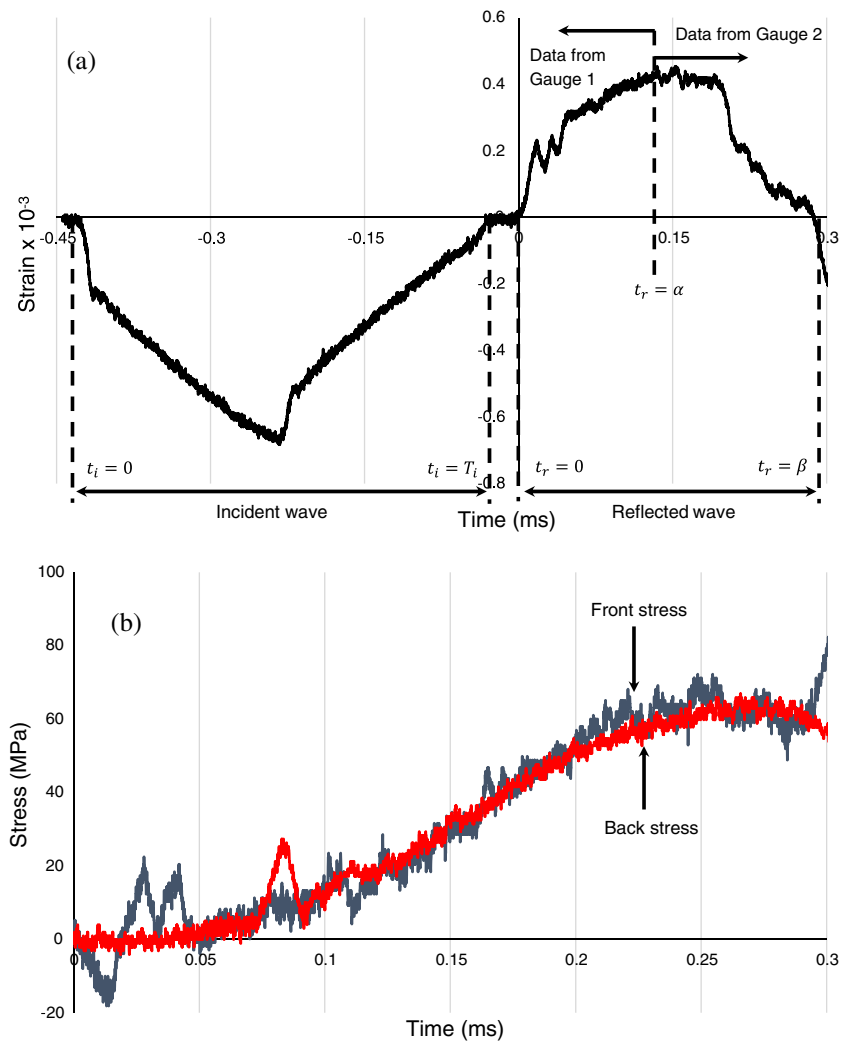
Data Processing from Gauge 2

The overlapping of incident and reflected pulses are observed to occur at Gauge 2. This superpositioning is present at the end of the incident and beginning of the reflected signal. From equation (8), the valid time interval for the reflected wave where overlapping does not occur is calculated as $0.11 \times 10^{-3} s \leq t_r \leq 0.29 \times 10^{-3} s$, which is visualized in Fig. 5(a). As expected, the front and back stress history of the specimen is unsynchronized prior a time of 0.11 ms (Fig. 5(b)).

Wave Collation

Fig. 6(a) shows the complete reconstructed strain history created from data collected at Gauges 1 and 2 as per equation (11) with the positions of α and β delineated. Comparison between the front and rear specimen stresses (Fig. 6(b)) subsequently indicates that excellent dynamic stress equilibrium is achieved for $t_r \leq \beta$, enabling the derivation of the dynamic stress-strain response and strain rate of the specimen (Fig. 7). The linear stress-strain response observed for dry silica sand up to

Fig. 6 Incident and reflected wave history (a) and comparison between specimen front and rear stresses (b) for strains reconstructed from Gauges 1 and 2 via the wave collation technique



60 MPa at high rates of strain is consistently reported throughout literature [8, 9, 12, 20], which confirms the veracity of the extracted result. It is therefore experimentally demonstrated that the wave collation technique is a valid solution for the elimination of wave overlapping effects occurring in short incident bars.

Finite Element Validation

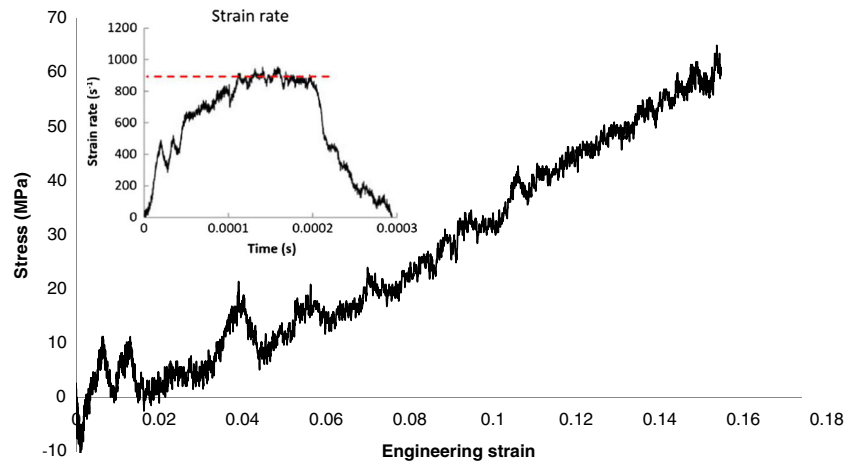
Finite element (FE) analyses have been established as an invaluable tool for the simulation of stress wave propagation in Hopkinson bar tests [21]. To numerically validate the wave collation technique employed in Section 2.2, a full 3D FE model of the SHPB setup described in the preceding section is constructed in Abaqus/Explicit [22]. The mesh comprises of reduced-integration linear hexahedral elements (C3D8R) with an average size of 2 mm, resulting in a total of 80,880 elements sufficient to obtain a converged solution. The incident and transmission bars are modeled via an isotropic elastic

material model with $E = 210$ GPa, $\rho = 7800$ kg/m³ and $\nu = 0.3$. The incident wave shown in Fig. 4(a) was applied to the impact end of the incident bar as a stress pulse.

In order to numerically validate the proposed wave collation technique, the expected dynamic specimen response is required. The Crushable Foam material model with volumetric hardening is therefore adopted, which mimics compaction with confinement of the sand specimen by limiting lateral expansion [22]. The elastic material parameters implemented are $E = 40$ GPa, $\rho = 1540$ kg/m³ and $\nu = 0.0$. The compression and hydrostatic yield stress ratio is taken as $k = 1$ and $k_t = 0.1$ respectively, which is adequate for a material response dominated by compressive stress [23]. The material hardening input curve is derived from the experiment as shown in Fig. 7.

As illustrated via Fig. 8(a), the FE simulations correlate exceptionally well with experimental waves and are able to successfully capture the superpositioning effect at both gauges. This confirms that the material model and input parameters adopted here are appropriate to reproduce the experimental mechanical response of the sand specimen with the

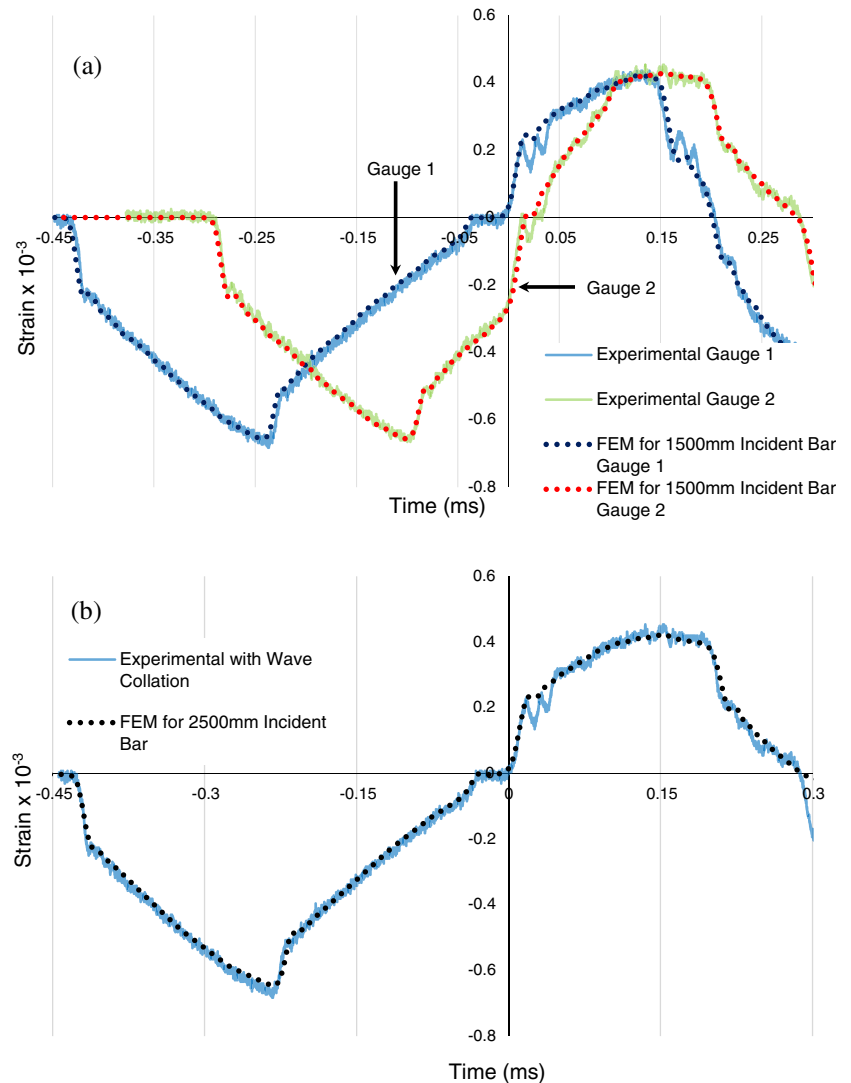
Fig. 7 Dynamic stress-strain behavior of sand specimen at a strain rate of 900 s^{-1} extracted via the wave collation technique



purpose of validating the proposed wave collation technique. The 1500 mm incident bar is subsequently extended to 2500 mm and converted into a typical single gauge setup

(gauge is located at 1100 mm from the specimen/incident bar interface) in the FE model. This allows for the observation of true incident and reflected wave histories without

Fig. 8 (a) Comparison between experimental and FE strain histories recorded at Gauges 1 and 2 and (b) after wave collation



necessitating the proposed wave collation (the simulated incident bar is now of sufficient length to capture non-overlapping wave propagation). A comparison of the numerical results with experimental signals reconstructed from Gauges 1 and 2 (Fig. 8(b)) demonstrates excellent synchronicity thus confirming the validity of the wave collation technique.

Discussion and Applications

The proposed technique of wave collation is intended for situations where the overlapping of incident and reflected stress waves occur in an incident bar that is unable to accommodate the full duration of a given input pulse. The method is designed as a rapid and direct approach to the wave superpositioning issue intermittently encountered by researchers working with the SHPB. The technique addresses situations where the loading pulse duration is dramatically increased due to pulse shaping and/or usage of a long striker bar in order to facilitate dynamic stress equilibrium and constant rate deformations in the specimen. Additionally, the method is most desirable under high strain rate conditions beyond 1000 s^{-1} where sufficient specimen strains are generally able to be attained. Thus, the extraction of valid experimental data is made possible without alterations to the existing setup of the bars, which may prove impractical from an economic or logistical standpoint due to possible constraints within the testing environment. However, as the described method only considers a single wave reflection in the incident bar, it may be unable to satisfy situations where very high specimen strains are desired. The implementation of optimized multi-strain/multi-velocity wave separation techniques is therefore required for such proposes [18]. Furthermore, the collation technique is most effective when wave dispersion is significantly minimized such as with the use of pulse shaping and numerical correction of the wave dispersion is not necessary [6]. The presence of dispersion could compromise the amalgamation of strain data influenced by the relative positioning of the two gauges. Nevertheless, the wave collation approach is effective at suppressing wave overlapping at lower strains for non-dispersive SHPB experiments for which tests can be easily designed to accommodate (Fig. 3). Ultimately, the inherently simplistic nature of the technique underlines its accessibility to technicians and experimentalists across a broad spectrum of technical expertise.

Conclusions

A collation technique for the mitigation of wave overlapping in the incident bar for the SHPB is proposed. The method is beneficial for high strain rate SHPB testing situations where a longer incident bar is unavailable or impractical. A complete

incident and reflected strain history for a single wave reflection can be created via reconstructing the strains extracted from gauges attached at two distinct locations on the incident bar. Experimental testing on a sand specimen with pulse shaping confirmed that the requirements of dynamic stress equilibrium and non-overlapping wave propagation can be satisfied with this method. Finite element simulations utilizing a sufficiently long incident bar to suppress signal overlap further confirmed its veracity. The proposed wave collation technique therefore presents an effective alternative for the extraction of complete strain histories of the incident and reflected pulse if the incident bar is insufficiently long to prevent the superpositioning of wave trains.

Acknowledgements This work was supported in part by the Australian Research Council through Discovery Projects (DP140100945), by the Faculty of Engineering & Information Technologies at The University of Sydney through the Faculty Research Cluster Program, and by the National Natural Science Foundation of China through Grant No. 11232003.

References

1. Field JE, Walley SM, Proud WG, Goldrein HT, Siviour CR (2004) Review of experimental techniques for high rate deformation and shock studies. *Int J Impact Eng* 30:725–775
2. Bragov AM, Grushevsky GM, Lomunov AK (1996) Use of the Kolsky method for confined tests of soft soils. *Exp Mech* 36:237–242
3. Omidvar M, Iskander M, Bless S (2012) Stress-strain behavior of sand at high strain rates. *Int J Impact Eng* 49:192–213
4. Hopkinson B (1913) A method of measuring the pressure produced in the detonation of high explosives or by the impact of bullets. *Philos Trans R Soc London, Ser A* 213:437–456
5. Kolsky H (1949) An investigation of the mechanical properties of materials at very high rates of loading. *Proc R Soc Lond Ser B* 62: 676–700
6. Chen W, Song B (2011) *Split Hopkinson (Kolsky) Bar Design, Testing and Applications*. Springer, New York
7. Lindholm US (1964) Some experiments with the split hopkinson pressure bar. *J Mech Phys Solids* 12:317–335
8. Martin BE, Chen W (2009) The high-rate behavior of a fine grain sand. In: *Proceedings of the SEM Annual Conference*. Society for Experimental Mechanics Inc., Albuquerque
9. Song B, Chen W, Luk V (2009) Impact compressive response of dry sand. *Mech Mater* 41:777–785
10. Frew DJ, Forrestal MJ, Chen W (2002) Pulse shaping techniques for testing brittle materials with a split hopkinson pressure bar. *Exp Mech* 42:93–106
11. Hiermaier S, Meenken T (2010) Characterization of low-impedance materials at elevated strain rates. *J Strain Anal Eng Des* 45:401–409
12. Martin BE, Chen W, Song B, Akers SA (2009) Moisture effects on the high strain-rate behavior of sand. *Mech Mater* 41:786–798
13. Lundberg B, Henchoz A (1977) Analysis of elastic waves from two-point strain measurement. *Exp Mech* 17:213–218
14. Follansbee PS, Frantz C (1983) Wave propagation in the split hopkinson pressure bar. *J Eng Mater Technol* 105:61–66
15. Zhao H, Gary G (1997) A new method for the separation of waves. Application to the SHPB technique for an unlimited duration of measurement. *J Mech Phys Solids* 45:1185–1202

16. Pochhammer L (1876) On the propagation velocities of small oscillations in an unlimited isotropic circular cylinder. *J Reine Angew Math* 81:324–326
17. Chree C (1889) The equations of an isotropic elastic solid in polar and cylindrical coordinates, their solutions and applications. *Trans Cambridge Philos Soc* 14:250–369
18. Bussac M-N, Collet P, Gary G, Othman R (2002) An optimisation method for separating and rebuilding one-dimensional dispersive waves from multi-point measurements. Application to elastic or viscoelastic bars. *J Mech Phys Solids* 50:321–349
19. Othman R, Guegan P, Challita G, Pasco F, LeBreton D (2009) A modified servo-hydraulic machine for testing at intermediate strain rates. *Int J Impact Eng* 36:460–467
20. Luo H, Lu H, Cooper WL, Komanduri R (2011) Effect of mass density on the compressive behavior of dry sand under confinement at high strain rates. *Exp Mech* 51:1499–1510
21. Ramirez H, Rubio-Gonzalez C (2006) Finite-element simulation of wave propagation and dispersion in Hopkinson bar test. *Mater Des* 27:36–44
22. Abaqus Analysis User's Manual (Version 6.13) (2013). Dassault Systemes Simulia Corp
23. Flores-Johnson EA, Li QM (2012) Structural behaviour of composite sandwich panels with plain and fibre-reinforced foamed concrete cores and corrugated steel faces. *Compos Struct* 94:1555–1563